NeuroImage **13,** 751–758 (2001)
doi:10.1006/nimg.2000.0719, available online at http://www.idealibrary.com on IDEAL®

Removal of Confounding Effects of Global Signal in Functional MRI Analyses[1]

Adrien E. Desjardins, Kent A. Kiehl, and Peter F. Liddle

Neuroimaging Laboratory, Department of Psychiatry, University of British Columbia, Vancouver, British Columbia, Canada V6T 2A1

Received June 13, 2000

Local signals obtained from BOLD fMRI are generally confounded by global effects. In this paper, we make an essential distinction between global effects and the global signal. Global effects have a similar influence on local signals from a large proportion of cerebral voxels. They may reflect diffuse physiological processes or variations in scanner sensitivity and are difficult to measure directly. Global effects are often estimated from the global signal, which is the spatial average of local signals from all cerebral voxels. If the global signal is strongly correlated with experimental manipulations, meaningfully different results may be obtained whether or not global effects are modeled (G. K. Aguirre *et al.*, 1998, *NeuroImage,* 8, 302–306). In particular, if local BOLD signals make a significant contribution to the global signal, analyses using ANCOVA or proportional scaling models may yield artifactual deactivations. In this paper, we present a modification to the proportional scaling model that accounts for the contribution of local BOLD signals to the global signal. An event-related oddball stimulus paradigm and a block design working memory task were used to illustrate the efficacy of our model.

INTRODUCTION

Functional magnetic resonance imaging (fMRI) is used to identify local hemodynamic responses invoked by experimentally controlled stimuli. Typically, in the case of blood oxygen level-dependent (BOLD) fMRI, a large cerebral volume is imaged, and statistical analyses are performed on signals from subcomponents of this volume to test hypotheses regarding changes in neural activity. In this paper, we assume that analyses are performed with the general linear model (Friston *et al.*, 1995b,c; Worsley and Friston, 1995).

A variety of global effects can interfere with the detection of local BOLD signals. Their origins include underlying physiological processes, gross body movements, physiological movements (pulsations, swallowing, abdominal movements, breathing), and long-term instabilities of the scanner baseline (Friston, 1996; Kruggel, 1999). In an ANCOVA model, global effects are treated as additive effects that do not affect local BOLD signals or error variances. In a proportional scaling model, they are treated as gain effects that equally affect all local BOLD signals and error variances. An assumption contained in both models is that global effects are not correlated with the covariates of interest. Global effects are often estimated from the global signal, the spatial average of local signals from all cerebral voxels. Note that the terms *global effects* and *global signal* are sometimes used interchangeably in the literature; the distinction is crucial for the purposes of this paper.

If the global signal is strongly correlated with experimental manipulations, meaningfully different results may be obtained whether or not global effects are modeled (Aguirre *et al.*, 1998). Similar problems have been encountered in analyses of positron emission tomography (PET) activation images (Andersson, 1997). Strong correlations between the global signal and experimental manipulations can reflect the contribution of local BOLD signals to the global signal. If this contribution is significant, it is likely that the global signal is also strongly correlated with the covariates of interest. In the context of PET, Andersson (1997) proposed using a modified global signal calculated only from voxels that are weakly correlated with the covariates of interest. This method may not be appropriate for fMRI given the greater sensitivity of fMRI compared with PET.

In this paper, we present a modification to the proportional scaling model that accounts for the contribution of local BOLD signals to the global signal. In our model, an *adjusted global signal* replaces the global signal. The adjusted global signal is calculated by or-

[1] The code for implementing adjusted proportional scaling in SPM 99 analyses is available on request from Peter F. Liddle, 2255 Wesbrook Mall, Department of Psychiatry, University of British Columbia, Vancouver, BC, Canada, V6T 2A1. Fax: (604) 822-7756. E-mail: liddle@interchange.ubc.ca.

1053-8119/01 $35.00

thogonalizing the global signal with respect to nonconstant covariates of the experimental design matrix. The use of the adjusted global signal is justified by the following arguments. In the proportional scaling model, the assumed form for the local signal from voxel i, $I_i(t)$, is

$$I_i(t) = G(t)[\mu_i + \boldsymbol{\alpha}_i \cdot \boldsymbol{h}(t) + \boldsymbol{\beta}_i \cdot \boldsymbol{c}(t) + \epsilon_i(t)], \quad (1)$$

where t is a discrete time variable (e.g., scan number) and $G(t)$ is the multiplicative factor arising from global effects. $\boldsymbol{h}(t) = [h_1(t) \ldots h_P(t)]'$ and $\boldsymbol{c}(t) = [c_1(t) \ldots c_Q(t)]'$ are vectors of covariates that represent the BOLD signal invoked by experimental manipulations (the covariates of interest) and the local nuisance effects (the covariates of no interest), respectively. $\epsilon_i(t)$ is a normally distributed error term, $\epsilon_i(t) \sim N(0, \sigma_i^2)$; μ_i is the baseline intensity; and the parameter estimates $\boldsymbol{\alpha}_i$ and $\boldsymbol{\beta}_i$ are constant row vectors. Here we assume that $G(t)$ is uncorrelated with $\boldsymbol{h}(t)$ and $\boldsymbol{c}(t)$. By definition, the global signal is a spatial average of local signals from all cerebral voxels,

$$g(t) = \frac{1}{m} \sum_{i=1}^{m} I_i(t), \quad (2)$$

where m is the number of cerebral voxels. Defining $G_v(t)$ as the variation of $G(t)$ about its mean $\bar{G}$,

$$G(t) = \bar{G} + G_v(t), \quad (3)$$

and combining (1) and (2) gives

$$\begin{aligned} g(t) = \frac{1}{m} \sum_i \{(\bar{G} + G_v(t)) \cdot (\mu_i + \boldsymbol{\alpha}_i \cdot \boldsymbol{h}(t) \\ + \boldsymbol{\beta}_i \cdot \boldsymbol{c}(t) + \epsilon_i(t))\} = \left[(\bar{G} + G_v(t)) \frac{1}{m} \sum_i \mu_i \right] \\ + \left[\bar{G} \frac{1}{m} \sum_i (\boldsymbol{\alpha}_i \cdot \boldsymbol{h}(t) + \boldsymbol{\beta}_i \cdot \boldsymbol{c}(t)) \right] \\ + \left[\frac{1}{m} \sum_i (G_v(t)\boldsymbol{\alpha}_i \cdot \boldsymbol{h}(t) + G_v(t)\boldsymbol{\beta}_i \cdot \boldsymbol{c}(t)) \right] \\ + \left[(\bar{G} + G_v(t)) \frac{1}{m} \sum_i \epsilon_i(t) \right]. \end{aligned} \quad (4)$$

The first term in square brackets in Eq. (4) is the average baseline intensity scaled by $G(t)$. The second term, a linear combination of nonconstant covariates of the experimental design matrix, is removed by orthogonalization. The third term is a spatial average of the interactions between $G_v(t)$ and the local BOLD and nuisance effects. This term is a negligible second-order effect if $G_v(t)$ and the nuisance effects are both small relative to G or if the interactions are incoherent and cancel out in the spatial average (note that the fractional change in signal due to the BOLD effect is always small—typically less than 5%). We verified this condition for both experiments. We assume that the last term, the spatial average of the error terms scaled by $G(t)$, is negligible. Under the assumptions above, the adjusted global signal, $g_a(t)$, is proportional to $G(t)$,

$$g_a(t) = (\bar{G} + G_v(t)) \frac{1}{m} \sum_i \mu_i = G(t)B, \quad (5)$$

where B is the average baseline intensity. Scaling local signals by the adjusted global signal prior to analysis produces signals of the form assumed by the general linear model (B is inconsequential in subsequent analyses):

$$I_i(t)/g_a(t) = [\mu_i + \boldsymbol{\alpha}_i \cdot \boldsymbol{h}(t) + \boldsymbol{\beta}_i \cdot \boldsymbol{c}(t) + \epsilon_i(t)]/B. \quad (6)$$

Data from two experiments were used to test this model: (1) an event-related oddball stimulus paradigm (Kiehl *et al.*, 2001; Kiehl and Liddle, 2001) and (2) a block-design working memory task (Mendrek *et al.*, in preparation). Three analyses were performed on the data, in which (i) local signals were not scaled, (ii) local signals were scaled by the global signal (proportional scaling), and (iii) local signals were scaled by the adjusted global signal (adjusted proportional scaling).

MATERIALS AND METHODS

Experiment 1

Image volumes were collected from six male and four female right-handed healthy participants (mean age 24.2 years). Two sets of 244 auditory stimuli were presented to each participant by a computer-controlled auditory sound system via insert earphones. Nontarget, target, and novel stimuli consisted of 1000-Hz tones, 1500-Hz tones, and nonrepeating random noises, respectively. The duration of each stimulus was 200 ms, the interstimulus interval (ISI), 2000 ms. Participants were instructed to press a button with their right index finger as soon as they heard a target stimulus and not to respond to a nontarget or novel stimulus. The stimulus paradigm and data acquisition techniques are described more fully in Kiehl *et al.* (2001) and Kiehl and Liddle (2001).

Imaging was performed with a clinical GE 1.5-T scanner fitted with a Horizon Echo-Speed upgrade. Functional image volumes were collected with a gradient-echo sequence (TR/TE 3000/40 ms, flip angle 90°, FOV 24 × 24 cm, 64 × 64 matrix, 62.5-kHz bandwidth,

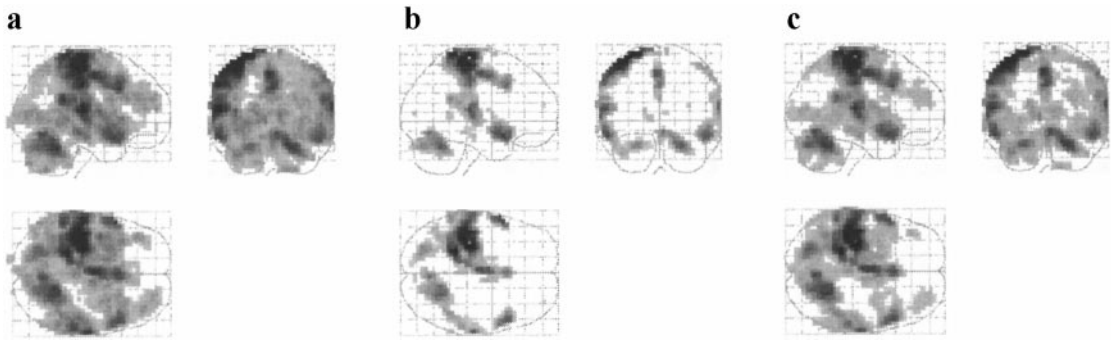

FIG. 1. SPM{*t*}'s for target responses obtained from analyses with (a) no scaling, (b) proportional scaling, and (c) adjusted proportional scaling. The data are presented as a maximum intensity projection (MIP) on a standard template brain. In the MIP, the three views are presented: sagittal, coronal, and transverse. The gray scale is arbitrary and all SPM{*t*}'s are set at a corrected voxel-level threshold of $P < 0.05$. Note the similarities between SPM{*t*}'s from the analyses without scaling and with adjusted proportional scaling. The analysis with proportional scaling yielded considerably fewer activations. *Z* scores were highest overall in the analysis with adjusted proportional scaling and lowest overall in the analysis with proportional scaling.

3.75 by 3.75-mm in-plane resolution, 5-mm slice thickness, 29 slices) effectively covering the entire brain (145 mm). During each stimulus run, 167 image volumes were acquired. The first 4 were collected to allow T_1 effects to stabilize and were not included in subsequent analyses.

Sessional realignment (Friston *et al.*, 1995a, 1996), nonlinear spatial normalization (Friston *et al.*, 1995a), and spatial smoothing (Gaussian kernel, FWHM = $8 \times 8 \times 8$ mm) were performed with the software Statistical Parametric Mapping 99 (Wellcome Department of Cognitive Neurology). In analyses without proportional or adjusted proportional scaling, image volumes from each session were scaled by the corresponding mean global signals to compensate for sessional intensity variations. To remove low-frequency and high-frequency confounds, a high-pass frequency filter (cutoff frequency 0.0088 Hz for odd-numbered sessions, 0.0093 Hz for even-numbered sessions) and a low-pass frequency filter (cutoff frequency 0.158 Hz) were applied. Hemodynamic responses to the target and novel stimuli were modeled using a synthetic response function composed of two gamma functions and a term proportional to its derivative (for the mathematical model, see Josephs *et al.*, 1997; for an illustration, see Friston *et al.*, 1998). The latter term was included to model small latency variations. It was assumed that responses to the frequent nontarget stimuli formed a constant baseline, so they were not modeled explicitly. The statistical significance of effects was tested using the modified Bonferroni correction for multiple comparisons described by Friston *et al.* (1995c), as implemented in SPM 99.

Experiment 2

Image volumes were collected from nine male and three female right-handed healthy participants (mean age 27.5 years). Two 7-min runs of visual stimuli were presented to each participant by a computer-controlled video projection system. The stimuli consisted of letters presented for 250 ms, with an ISI of 2000 ms. Two conditions, "0-back" and "2-back," were presented separately in alternating 30-s periods separated by 20-s periods of rest. During the 0-back condition, participants were instructed to press the button with their

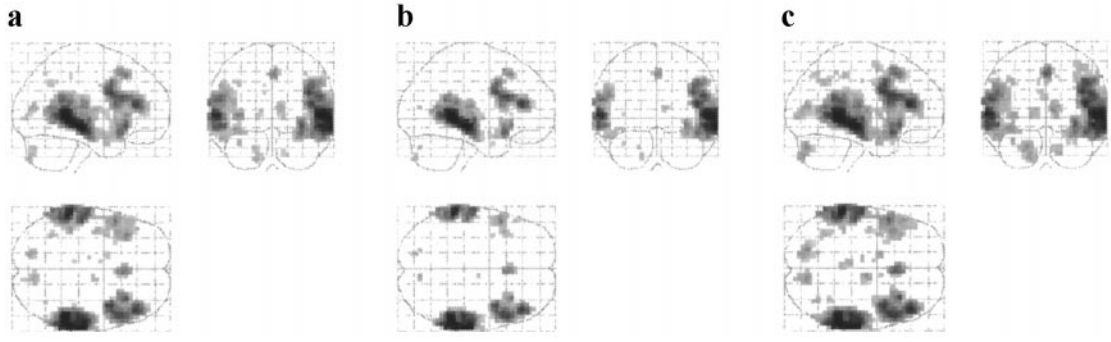

FIG. 2. SPM{*t*}'s for novel activations obtained from analyses with (a) no scaling, (b) proportional scaling, and (c) adjusted proportional scaling. The data are presented in the same manner as in Fig. 1. The similarities in activation patterns are consistent with the low correlation between the global signal and the novel covariate. *Z* scores were similar in all three analyses.

TABLE 1

Representative *Z* Scores from Experiment 1

Location [*x y z*]	*Z* scores from analyses of target responses relative to baseline		
	No scaling	Proportional scaling	Adjusted proportional scaling
Right anterior temporal lobe [48 16 −16]	10.98	9.87	11.42
Left anterior temporal lobe [−56 12 −16]	11.59	10.90	12.28
Supplementary motor area [−4 −12 52]	12.79	10.39	13.17
Right cerebellum [16 −56 −24]	12.60	9.26	12.62

right index finger when they saw an "X" appearing in the sequence of letters. In the 2-back condition, participants were instructed to press the button when they saw a letter that was identical to one presented two trials back. Both conditions involved similar sensory processing of information and a similar amount of motor activity. This task has been used in previous neuroimaging investigations of working memory (e.g., Awh *et al.*, 1996; Cohen *et al.*, 1997; Jonides *et al.*, 1997). A high-pass frequency filter (cutoff frequency 0.0033 Hz) and a low-pass frequency filter (cutoff frequency 0.158 Hz) were applied to remove low-frequency and high-frequency confounds, respectively. Additional imaging parameters and image preprocessing methods were the same as those employed in Experiment 1.

RESULTS AND DISCUSSION

In Figs. 1 and 2, we present thresholded SPM{*t*}'s from analyses of hemodynamic responses due to target and novel stimuli relative to baseline stimulus responses. In both cases, activations were more extensive in analyses without scaling and with adjusted proportional scaling than in the analyses with proportional scaling. Very similar activation patterns were observed from analyses without scaling and with adjusted proportional scaling, but *Z* scores from the latter analyses were higher overall. *Z* scores from analyses with proportional scaling were lowest overall. Representative *Z* scores from the three analyses are listed in Table 1.

The correlation between the global signal and the target covariate was high ($Z = 7.88$). Under the assumption that this correlation reflects contributions from local BOLD signals, it is consistent with the large extent of activation obtained from the analysis without scaling. In contrast, the correlation between the global signal and the novel covariate was low ($Z = 1.84$). The activation extent and *Z* scores obtained from all three analyses of novel responses relative to baseline were similar (see Fig. 2). The global signal from a representative session in Experiment 1 is shown in Fig. 3. The standard deviation of the global signal was 0.157% of the mean. In contrast, the standard deviation of the difference between the global signal and the adjusted signal was only 0.0328%. This indicates that the large high-frequency variations in the former signal are also present in the latter. The precise origin of these variations is unclear. Under the hypotheses of the proportional scaling model, however, such knowledge is un-

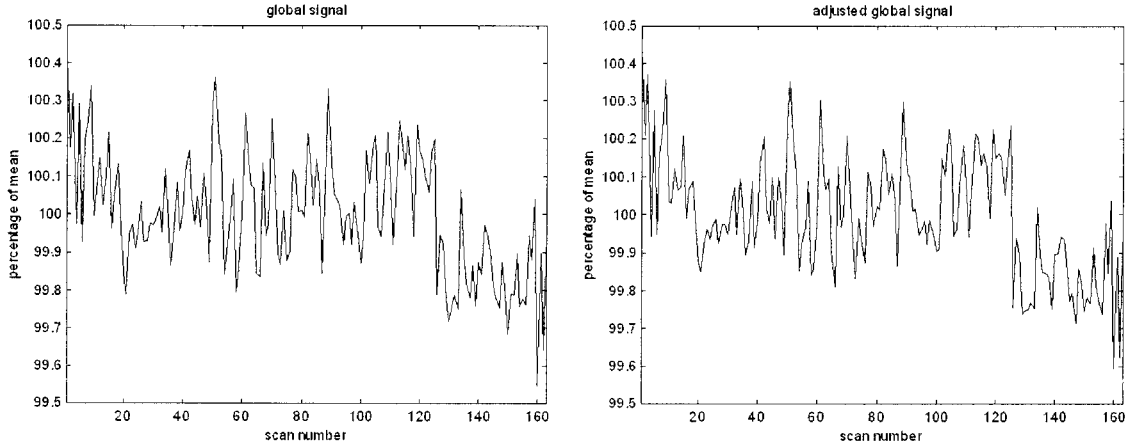

FIG. 3. Global signal and adjusted global signal of a representative session from Experiment 1. The standard deviation of the global signal is 0.157% of the mean. These graphs illustrate that the component of the global signal that was removed by orthogonalization with respect to the nonconstant covariates of interest was small relative to the variations about the mean: the standard deviation of the difference between the global signal and the adjusted global signal is only 0.0328%. See text for details.

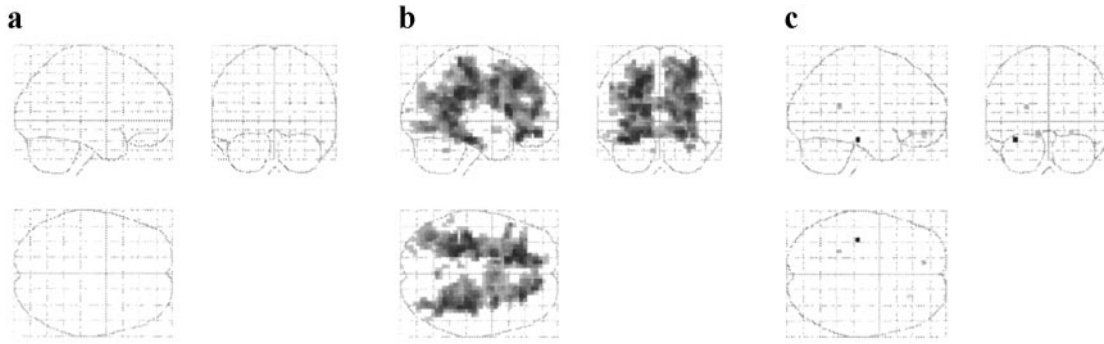

FIG. 4. SPM{*t*}'s for target deactivations obtained from analyses with (a) no scaling, (b) proportional scaling, and (c) adjusted proportional scaling. The data are presented in the same manner as in Fig. 1. The extensive white-matter deactivations shown in (b) are a direct result of the high correlations between the global signal and the target covariate. They are absent in both (a) and (c).

necessary for accurate measurements of local BOLD signals.

In Fig. 4, we present thresholded SPM{*t*}'s from analyses of deactivations during processing of targets relative to baseline. As expected from the high correlation between the global signal and the target covariate, the analysis with proportional scaling yielded extensive deactivations, primarily in white-matter voxels. These deactivations may safely be considered artifactual, and they are absent at a statistically significant level in the analyses without scaling and with adjusted proportional scaling. In this study, the large negative responses relative to baseline obtained from the analysis with proportional scaling illustrate the dramatic result of scaling a local signal that is uncorrelated with the covariates of interest by a highly correlated global signal, an effect well described by Aguirre *et al.* (1998).

A similar effect was observed in analyses of novel responses relative to target stimulus responses. The corresponding SPM{*t*}'s are shown in Fig. 5. The analysis with proportional scaling yielded the highest *Z* scores of the three analyses overall. In large part, the differences between conditions in white-matter voxels were artifactually induced by proportional scaling. We hypothesize from this result that the differences between conditions in gray-matter voxels were erroneously enhanced by proportional scaling. The differences between conditions obtained from the analysis with adjusted proportional scaling are consistent with the distribution of neural sources associated with novel stimuli from intracranial recordings and from data from patients with brain damage (Halgren *et al.*, 1995a,b, 1998; Knight, 1984; Knight and Nakada, 1998), although an exact comparison is not possible. While activations obtained from the analysis with adjusted proportional scaling were more extensive than those obtained from the analysis without scaling, similar patterns were obtained when slightly lower thresholds were used. These results suggest that the analysis with adjusted proportional scaling provided the most realistic account of novel responses relative to target stimulus responses.

The widespread activation in response to target stimuli may be surprising in view of the relative simplicity of the task. However, this observation is consistent with numerous reports of widespread activation during intracranial recordings of target stimuli from oddball studies in patients (Halgren and Marinkovic, 1996; Halgren *et al.*, 1998). This issue is discussed in greater detail by Kiehl *et al.* (2001) and Kiehl and Liddle (2001); other relevant papers include Mesulam (1990, 1994) and Mesulam *et al.* (1999).

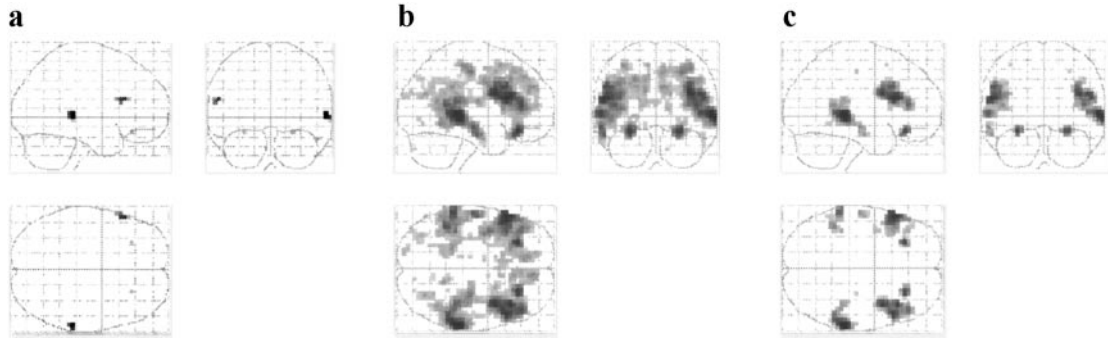

FIG. 5. SPM{*t*}'s for novel responses relative to target responses obtained from analyses with (a) no scaling, (b) proportional scaling, and (c) adjusted proportional scaling. The data are presented in the same manner as in Fig. 1. See text for details.

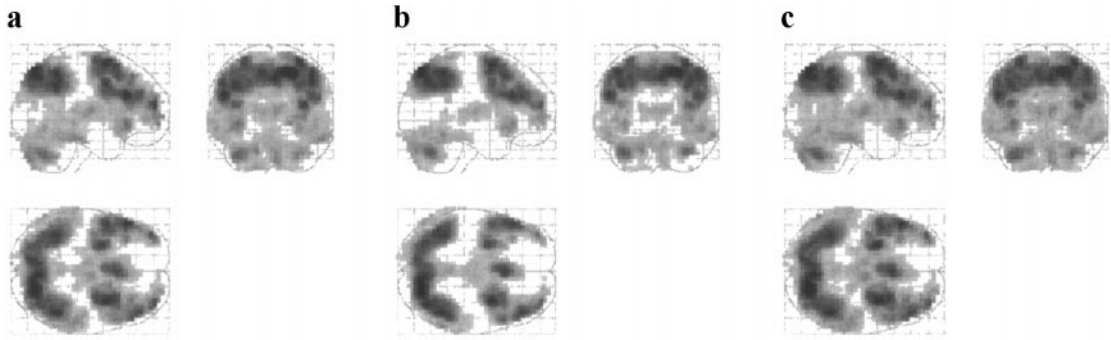

FIG. 6. SPM{*t*}'s for 2-back responses relative to the 0-back responses obtained from analyses with (a) no scaling, (b) proportional scaling, and (c) adjusted proportional scaling. The data are presented in the same manner as in Fig. 1. Note the similarities between SPM{*t*}'s from the analyses without scaling and with adjusted proportional scaling. The analysis with proportional scaling yielded a smaller activation extent. *Z* scores were highest overall in the analysis with adjusted proportional scaling and lowest overall in the analysis without scaling.

The results of Experiment 2 afford an independent test of the three analysis methods. We observed very different activation extents for the 2-back conditions and the 0-back conditions in analyses without scaling. For brevity, we present only SPM{*t*}'s corresponding to differences between the two conditions.

In Fig. 6, we present thresholded SPM{*t*}'s from analyses of 2-back responses relative to 0-back responses. Activations were more extensive in analyses without scaling and with adjusted proportional scaling than in the analyses with proportional scaling. Very similar activation patterns and *Z* scores were observed from analyses without scaling and analyses with adjusted proportional scaling. *Z* scores from analyses with adjusted proportional scaling were highest overall. Representative *Z* scores from the three analyses are listed in Table 2. The correlations between the global signal and the covariates of interest were large ($Z = 5.31$ for 2-back responses relative to 0-back responses). Under the assumption that this correlation primarily reflects contributions from local BOLD signals to the global signal, it is consistent with the large activation extent obtained from the analysis without scaling.

SPM{*t*}'s from analyses of 0-back responses relative to 2-back responses are shown in Fig. 7. For analyses without scaling, the extent of these deactivations is smaller than the extent of activations. This difference reflects the more demanding nature of the 2-back task. Similar deactivation patterns were reported in PET studies employing the *N*-back task (e.g., Awh *et al.*, 1996; Schumacher, 1996; Jonides *et al.*, 1997). The analysis with proportional scaling yielded extensive deactivations in white-matter voxels. These white-matter deactivations are consistent with the high correlation between the global signal and the covariates of interest and may safely be considered artifactual. They are absent in the analyses without scaling and adjusted proportional scaling.

In general, the correlation between the global signal and the experimental manipulations may be affected not only by the sum of local BOLD signals, but also by any mechanism or artifact that induces correlations between local signals and experimental manipulations. Movement-related artifacts are possible candidates. If the contribution of local BOLD signals is not the dominant one, orthogonalization of the global signal with respect to nonconstant covariates of the experimental design matrix may not be appropriate. To make this statement more precise, we discuss two extensions of the proportional scaling model for local signals (Eq. (1)) to include correlations between the global signal and the covariates of interest that are not due to local BOLD signals. First, we assume that these correlations are ex-

TABLE 2

Representative *Z* Scores from Experiment 2

	Z scores from analyses of 2-back responses relative to 0-back responses		
Location [*x y z*]	Analysis without scaling	Analysis with proportional scaling	Analysis with adjusted proportional scaling
Right parietal lobe [20 −76 52]	35.22	39.41	42.87
Left parietal lobe [−40 −52 40]	27.31	27.67	33.48
Right lateral frontal cortex [44 36 28]	22.52	24.44	29.02
Left lateral frontal cortex [−52 24 28]	28.27	30.01	34.29

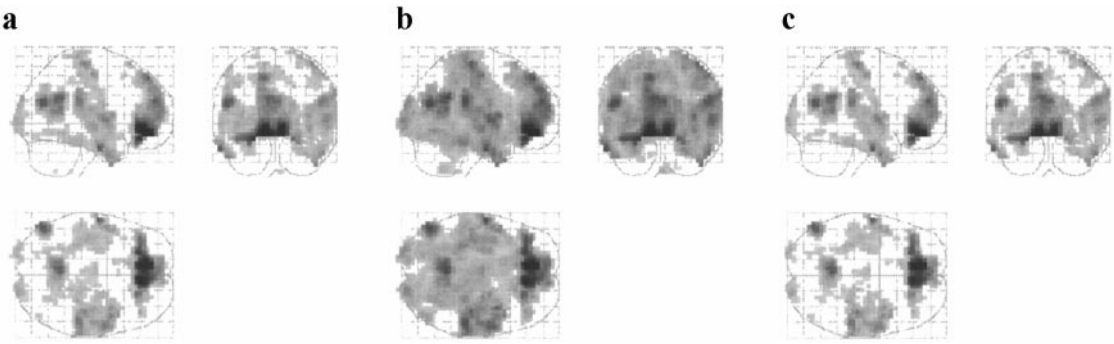

FIG. 7. SPM{*t*}'s for 0-back responses relative to 2-back responses obtained from analyses with (a) no scaling, (b) proportional scaling, and (c) adjusted proportional scaling. The data are presented in the same manner as in Fig. 1. The analysis with proportional scaling yielded extensive white-matter deactivations that are absent in both (a) and (c). See text for details.

pressed locally, so that they can be modeled by the inclusion of additive terms of the form $a_i(t)$, where $a_i(t)$ is significantly correlated with the covariates of interest:

$$I_i(t) = [\bar{G} + G_v(t)][\mu_i + \boldsymbol{\alpha}_i \cdot \boldsymbol{h}(t) + \boldsymbol{\beta}_i \cdot \boldsymbol{c}(t) + a_i(t) + \epsilon_i(t)]. \quad (7)$$

Here we assume that $G_v(t)$ is uncorrelated with the covariates of interest. Orthogonalization *is* appropriate: scaling local signals by the adjusted global signal calculated from Eq. (7) would remove variations due to $G_v(t)$ without introducing additional terms that are correlated with the covariates of interest. To accurately estimate local BOLD signals, however, methods for distinguishing between $a_i(t)$ and $\boldsymbol{\alpha}_i \cdot \boldsymbol{h}(t)$ are required. A discussion of such methods is given in Friston *et al.* (1996). A second possibility is that correlations between the global signal and the covariates of interest are induced by $G(t)$. In this case, orthogonalization may not be appropriate. We express the variation of $G(t)$ about its mean as the sum of terms $G_v(t)$ and $A(t)$ that are uncorrelated and correlated with the covariates of interest, respectively:

$$G(t) = \bar{G} + G_v(t) + A(t). \quad (8)$$

In this case, the local signals are given by

$$I_i(t) = [\bar{G} + G_v(t) + A(t)] \times [\mu_i + \boldsymbol{\alpha}_i \cdot \boldsymbol{h}(t) + \boldsymbol{\beta}_i \cdot \boldsymbol{c}(t) + \epsilon_i(t)]. \quad (9)$$

Under the assumptions that $G_v(t)$ and $A(t)$ are small relative to $\bar{G}$ and that products of the variations $G_v(t)$, $A(t)$, $\boldsymbol{\alpha}_i \cdot \boldsymbol{h}(t)$, and $\boldsymbol{\beta}_i \cdot \boldsymbol{c}(t)$ are negligible, the adjusted global signal and the scaled local signals are given by

$$g_a(t) = (\bar{G} + G_v(t)) \frac{1}{m} \sum_i \mu_i = [G(t) - A(t)]B \quad (10)$$

$$I_i(t)/g_a(t) = [\mu_i + \boldsymbol{\alpha}_i \cdot \boldsymbol{h}(t) + (\mu_i/\bar{G})A(t) + \boldsymbol{\beta}_i \cdot \boldsymbol{c}(t) + \epsilon_i(t)]/B, \quad (11)$$

where B is the average baseline intensity (the variation of the reciprocal term $1/g_a(t)$ was calculated using the approximation $(1 + \eta)^{-1} \approx 1 - \eta$, valid for $\eta \ll 1$). In subsequent analyses of Eq. (11), measurements of local BOLD signals would be artifactually augmented by additive terms of the form $(\mu_i/\bar{G})A(t) \approx A(t)$. In our analyses of Experiments 1 and 2, we made the conventional assumption that $G(t)$ is uncorrelated with the covariates of interest (Frackowiak *et al.*, 1997; Aguirre, 1998). More accurate characterizations of global effects are required to substantiate this assumption.

A proportional scaling model is appropriate for fMRI analyses when global effects can be attributed to gain effects that equally affect BOLD signals and error variance in local signals. In this context, orthogonalization of the global signal with respect to nonconstant covariates of the experimental design matrix is appropriate when global effects are not correlated with experimental manipulations. The contributions of local BOLD signals to the global signal may induce a strong correlation between the global signal and experimental manipulations. In this case, it is likely that the adjusted global signal is a better characterization of global effects than the global signal.

ACKNOWLEDGMENTS

We thank MR technicians Trudy Shaw, Karen Smith, and Sylvia Renneberg for their assistance. This research was supported in part by grants from the Norma Calder Society, the Medical Research

Council (MRC) of Canada, the British Columbia Health Services, and the British Columbia Medical Services Foundation and by funds from the Schizophrenia Division, Department of Psychiatry, University of British Columbia.

REFERENCES

Aguirre, G. K., Zarahn, E., and D'Esposito, M. 1998. The inferential impact of global signal covariates in functional neuroimaging analyses. *NeuroImage* **8:** 302–306.

Andersson, J. L. 1997. How to estimate global activity independent of changes in local activity. *NeuroImage* **6:** 237–244.

Awh, E., Jonides, J., Smith, E. E., Schumacher, E. H., Koeppe, R. A., and Katz, S. 1996. Dissociation of storage and rehearsal in verbal working memory. *Psychol. Sci.* **7:** 2531.

Cohen, J. D., Perlstein, W. M., Braver, T. S., *et al.* 1997. Temporal dynamics of brain activation during a working memory task. *Nature* **386:** 604–608.

Frackowiak, R. S. J., Friston, K. J., Frith, C. D., Dolan, R. J., and Mazziotta, J. C. 1997. *Human Brain Function,* pp. 59–84. Academic Press, San Diego.

Friston, K. J., Frith, C. D., Liddle, P. F., Dolan, R. J., Lammertsma, A. A., and Frackowiak, R. S. J. 1990. The relationship between global and local changes in PET scans. *J. Cereb. Blood Flow Metab.* **10:** 458–466.

Friston, K. J., Ashburner, J., Frith, C. D., Poline, J.-B., Heather, J. D., and Frackowiak, R. S. J. 1995a. Spatial registration and normalization of images. *Hum. Brain Mapp.* **2:** 165–189.

Friston, K. J., Holmes, A. P., Poline, J. B., Grasby, P. J., Williams, S. C., Frackowiak, R. S., and Turner, R. 1995b. Analysis of fMRI time-series revisited. *NeuroImage* **2:** 45–53.

Friston, K. J., Holmes, A. P., Worsley, K. J., Poline, J.-P., Frith, C. D., and Frackowiak, R. S. J. 1995c. Statistical parametric maps in functional imaging; A general linear approach. *Hum. Brain Mapp.* **2:** 189–210.

Friston, K. J., Williams, S., Howard, R., Frackowiak, R. S., and Turner, R. 1996. Movement-related effects in fMRI time-series. *Magn. Reson. Med.* **35:** 346–355.

Friston, K. J., Fletcher, P., Josephs, O., Holmes, A., Rugg, M. D., and Turner, R. 1998. Event-related fMRI: Characterizing differential responses. *NeuroImage* **7:** 30–40.

Halgren, E., Baudena, P., Clarke, J. M., Heit, G., Liégeois, C., Chauvel, P., and Musolino, A. 1995a. Intracerebral potentials to rare target and distractor auditory and visual stimuli. I. Superior temporal plane and parietal lobe. *Electroencephalogr. Clin. Neurophysiol.* **94:** 191–220.

Halgren, E., Baudena, P., Clarke, J. M., Heit, G., Marinkovic, K., Devaux, B., Vignal, J. P., and Biraben, A. 1995b. Intracerebral potentials to rare target and distractor auditory and visual stimuli. II. Medial, lateral and posterior temporal lobe. *Electroencephalogr. Clin. Neurophysiol.* **94:** 229–250.

Halgren, E., and Marinkovic, K. 1996. General principles for the physiology of cognition as suggested by intracranial ERPs. In *Recent Advances in Event-Related Brain Potential Research* (C. Ogura, Y. Koga, and M. Shimokochi, Eds.), pp. 1072–1084. Elsevier, Amsterdam.

Halgren, E., Marinkovic, K., and Chauvel, P. 1998. Generators of the late cognitive potentials in auditory and visual oddball tasks. *Electroencephalogr. Clin. Neurophysiol.* **106:** 156–164.

Jonides, J. E., Schumacher, E. H., Smith, E. E., Lauber, E. J., Awh, E., Minoshima, S., and Koeppe, R. 1997. Verbal working memory load affects regional brain activation as measured by PET. *J. Cognit. Neurosci.* **9:** 462–475.

Josephs, O., Turner, R., and Friston, K. 1997. Event-related fMRI. *Hum. Brain Mapp.* **5:** 1–7.

Kiehl, K. A., Laurens, K. R., Duty, T. L., Forster, B. B., and Liddle, P. F. 2001. Neural sources involved in auditory target detection and novelty processing: An event-related fMRI study. *Psychophysiology,* in press.

Kiehl, K. A., and Liddle, P. F. 2001. An event-related fMRI study of an auditory oddball task in schizophrenia. *Schizophrenia Res.,* in press.

Knight, R. T. 1984. Decreased response to novel stimuli after prefrontal lesions in man. *Electroencephalogr. Clin. Neurophysiol.* **59:** 9–20.

Knight, R. T., and Nakada, T. 1998. Cortico-limbic circuits and novelty: A review of EEG and blood flow data. *Rev. Neurosci.* **9:** 57–70.

Kruggel, F., von Cramon, D. Y., and Descombes, X. 1999. Comparison of filtering methods for fMRI datasets. *NeuroImage* **10:** 530–543.

Mesulam, M. M. 1990. Large-scale neurocognitive networks and distributed processing for attention, language, and memory. *Ann. Neurol.* **28:** 597–613.

Mesulam, M. M. 1994. Neurocognitive networks and selectively distributed processing. *Rev. Neurol.* **150:** 564–569.

Mesulam, M. M., Hyman, S. E., Hobson, J. A., and Silvestri, R. 1999. Brain and behavior. In *The Harvard Guide to Psychiatry* (A. M. Nicholi, Ed.), 3rd ed., pp. 101–167. Belknap Press, Cambridge, MA.

Worsley, K. J., and Friston, K. J. 1995. Analysis of fMRI time-series revisited—Again. *NeuroImage* **3:** 173–181.